Inflammation (2025) 48:3235–3251
https://doi.org/10.1007/s10753-025-02262-z

RESEARCH

ZAKα Induces Pyroptosis of Colonic Epithelium Via the Caspase-11/GSDMD Pathway to Aggravate Colitis

Song Li[1] · Mingfei Chen[1] · Sizhe Zheng[1] · Waresi Abudourexiti[1] · Feng Zhu[1] · Zhongyuan Wang[1] · Yanzhe Guo[1] · Zeqian Yu[1] · Zirui Yang[1] · Liang Zhang[2] · Chao Ding[3] · Jianfeng Gong[1]

Received: 26 November 2024 / Revised: 29 January 2025 / Accepted: 30 January 2025 / Published online: 24 February 2025

Abstract

ZAKα-driven ribotoxic stress response (RSR) has been shown to trigger diverse biological effects. Nevertheless, its role in the pathogenesis of ulcerative colitis (UC) remained unclear. This study aimed to determine the role of ZAKα in the development of UC. Our study found that ZAKα expression was significantly increased in colonic epithelium of UC patients and DSS-colitis mouse models. Moreover, the expression level of ZAKα mRNA showed a positive correlation with disease activity. In the colitis model, Vemurafenib, the ZAKα inhibitor, treatment reduced colonic inflammation and ameliorated intestinal mucosal barrier damage, while Anisomycin, the RSR agonist, showed the opposite effect. In vitro experiments demonstrated that Anisomycin induced pyroptosis instead of apoptosis in C26 cell line. Western blot analysis revealed that Anisomycin triggered pyroptosis via the Caspase-11/GSDMD pathway. Further animal studies confirmed that Vemurafenib downregulated this pathway, reducing colonic epithelial cell pyroptosis. Finally, blocking Caspase-11 reduced severity of DSS-induced colitis in Anisomycin-treated mice. In all, ZAKα seems to play a crucial role in the pathogenesis of colitis, as it promotes pyroptosis in colonic epithelial cells and exacerbates colitis in part by upregulating the Caspase-11/GSDMD axis.

Song Li and Mingfei Chen contributed equally to this work.

✉ Chao Ding
dingchao19910521@126.com

✉ Jianfeng Gong
gongjianfeng@nju.edu.cn

[1] Department of General Surgery, Jinling Hospital, Affiliated Hospital of Medical School, Nanjing University, No. 305 East Zhongshan Road, Nanjing 210002, China

[2] Department of Gastrointestinal Surgery, Xuzhou Central Hospital, Xuzhou Clinical School of Xuzhou Medical College, Jiangsu, China

[3] Department of General Surgery, Drum Tower Hospital, Affiliated Hospital of Medical School, Nanjing University, Nanjing, China

Graphical Abstract

ZAKα, the key kinase driving the ribotoxic stress response (RSR), is highly expressed in colonic epithelium of UC patients, and the activation of ZAKα can upregulate the Caspase-11/GSDMD pathway to induce pyroptosis in colonic epithelial cells.

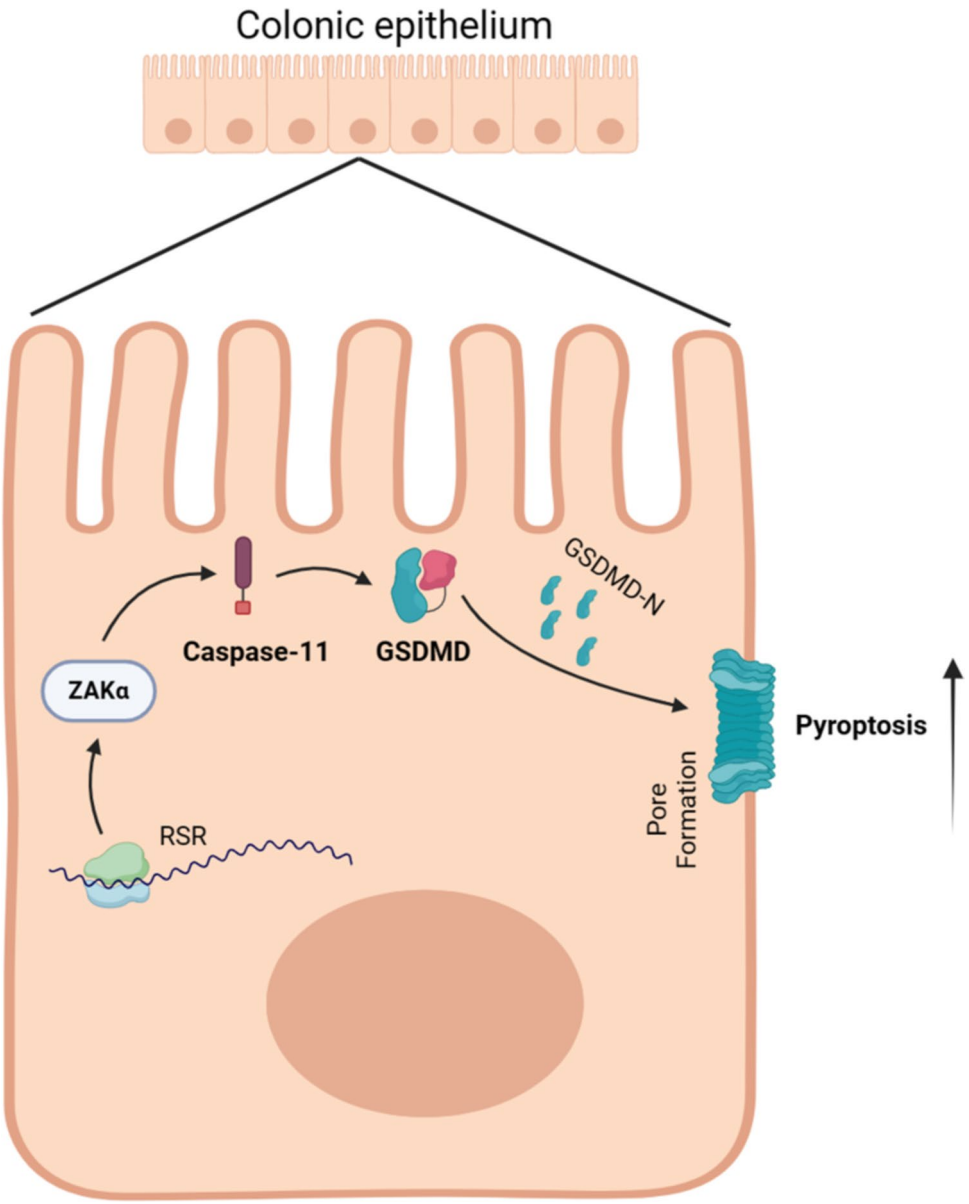

Keywords Ulcerative colitis · Ribotoxic stress response · ZAKα · Pyroptosis · Caspase-11

Introduction

Ulcerative colitis (UC) is a subtype of inflammatory bowel disease, characterized by lifelong inflammation impacting the rectum and colon to varying extents. Despite ongoing research, the exact etiology of UC remains elusive. It's commonly linked to genetic predispositions, environmental factors, compromised intestinal epithelial barriers, microbiota dysbiosis, and immune system irregularities [1].

Pyroptosis, as component of the innate immune response, acts as a cellular defense mechanism against extracellular pathogen-associated molecular patterns (PAMPs) and intracellular lipopolysaccharides (LPS). It operates through both canonical inflammasome-Caspase-1 pathway and non-canonical endogenous LPS-Caspase-4/5/11 pathways [2],

both activating the pyroptosis effector protein Gasdermin D (GSDMD) [3].

Pyroptosis played a significant role in UC. Katarzyna et al. found increased GSDMD in intestinal epithelium of IBD patients and experimental colitis mouse models, while mice lacking GSDMD exhibited reduced DSS-induced colitis [4]. Another study showed that UC patients exhibited higher levels of colonic Caspase-4 expression. Using inhibitors of Caspase-4/11 to alleviate exacerbated colitis due to the lack of the oxidative stress sensor glutathione peroxidase 8 (GPx8) further supported this finding [5]. IRG1/itaconic acid also played a protective role in DSS-induced colitis by inhibiting GSDMD/GSDME-mediated pyroptosis [6]. Additionally, the gut microbiota can induce macrophage pyroptosis and affect colitis. For example, *Desulfovibrio* and its flagellin protein exacerbated colitis by activating NAIP/NLRC4 inflammasomes to induce macrophage pyroptosis [7].

In 1997, Iordanov et al. discovered that inhibitors of the peptidyl transferase could bind to and damage 28S rRNA, thereby activating SAPK/JNK1 and described this process as ribotoxic stress response (RSR) [8]. ZAK (also named MLK7 or MRK) is a protein kinase belonging to the mixed lineage kinase (MLKs) family, and functionally classified as MAP3K, also known as MAP3K20. ZAK has two splice variants, namely ZAKα and ZAKβ [9–11], it also can activate JNK/p38 in response to anisomycin and UV radiation stimulation [12]. Of note, Thorpe et al. further demonstrated that ZAK plays a crucial role in mediating the activation of SAPKinases by intoxicated ribosomes, the specific subtype of ZAK involved remains unclear [13]. Subsequent studies revealed that this process was primarily mediated by ZAKα [14]. ZAKα contains ribosome binding domains (RBDs). When the 3' end function of 28S ribosomal RNA (rRNA) in the cell is disrupted due to various factors, leading to ribosomal stalling and collisions during translation, ZAKα perceives these stalling and collisions through its two C-terminal RBDs. Consequently, it undergoes autophosphorylation and activates downstream JNK/SAPK pathways, as well as the p38 MAPK signaling pathway. This process is referred to as the RSR [11, 14, 15]. ZAKα-driven RSR can induce various biological effects. For instance, the p38 MAPK signaling pathway, activated by ZAKα, can trigger cell cycle arrest, ultimately leading to apoptosis [16, 17]. Additionally, RSR play a role in metabolic regulation, where reactive oxygen species (ROS) generated during natural aging can trigger ribosomal damage and subsequent ZAKα activation, leading to metabolic abnormalities such as glucose intolerance, liver fibrosis, and white adipose tissue browning. In mice, deletion of the ZAK gene has been shown to mitigate futures of metabolic aging [18]. Moreover, RSR can modulate AMPK and mTOR signaling, affecting survival during starvation, stress hormone production, and blood glucose levels, thus regulating metabolic responses. $Zak^{-/-}$ mice typically exhibit a lean phenotype characterized by decreased body weight, reduced adipocyte size, increased browning of adipose tissue, and diminished liver fat content [19]. Of course, blocking RSR with kinase inhibitors demonstrates promising therapeutic potential for addressing certain pathological changes. For instance, the ZAK inhibitor DHP-2 effectively prevented anisomycin- and UV-induced apoptosis in COS-7 cells [12]. Additionally, other high-affinity ZAK inhibitors, such as sorafenib and nilotinib, were shown to inhibit doxorubicin-induced downregulation and apoptotic responses in HaCaT cells [20].

Previous studies have demonstrated that RSR can also induce pyroptosis. For example, Robinson et al. found that UV radiation can trigger RSR, subsequently driving hyperphosphorylation of the human-specific NLRP1 inflammasome ($NLRP1^{DR}$) directly through MAP3K20/ZAKα kinase and its downstream effector molecule p38, thereby promoting keratinocyte pyroptosis. Moreover, mutating a ZAKα phosphorylation site in $NLRP1^{DR}$ can abolish UV-induced pyroptosis [21]. Concurrently, a recent research has also discovered that toxins secreted by human diphtheria pathogens and nigericin from *Streptomyces hygroscopicus* can induce keratinocyte pyroptosis through this mechanism, partially elucidating certain aspects of the pathogenic mechanisms induced by these pathogens [22, 23]. Overall, the activation of ZAKα and its downstream p38/JNK appears to be closely associated with pyroptosis.

So far, the role of ZAKα in the development and progression of UC remains unknown. We hypothesized that ZAKα is activated in colonic tissues of UC patients, and may induce pyroptosis to aggravate colitis. The aim of this study is to investigate the status of ZAKα in colitis and its possible mechanisms.

Methods

Ethics Statement

This study was approved by the Ethics Committee of *Jinling* Hospital (2021NZKY-011–01). All animal procedures were performed in accordance with the guidelines of the Institutional Animal Care and Use Committee of *Jinling* Hospital.

Patients and Human Samples

All patients were recruited from the IBD center of *Jinling* Hospital between October 2022 through June 2023. Colonic tissues were collected from surgical specimen of UC patients. Control tissues were obtained from normal colon of colorectal cancer specimen. The inclusion and exclusion criteria are as follows: definite diagnosis of UC based on clinical, radiological, and endoscopic examination

and histological findings; while exclusion criteria involved patients who had taken RSR-interfering drugs within the past 4 weeks (such as Vemurafenib, Harringtonin, Adriamycin, and Daunorubicin, etc.). We included a total of 24 UC patients and 24 control samples, and found that the control group was significantly older than the UC group (58.73 ± 6.14 *vs* 41.43 ± 7.32; $p = 0.031$). The baseline characteristics are described in Supplementary Table 1.

Mice

Eight-week old C57BL/6 female mice were used. Mice were housed in specific pathogen-free (SPF) environment under controlled conditions: 23 ± 1 °C, 45–65% humidity, and a 12-h dark–light cycle, with unrestricted access to chow diet and water, unless specified otherwise.

To induce colitis, 2.5% DSS [36–50 kDa, MP Biomedicals] were orally administered for 7 consecutive days [24]. Moreover, mice were administered (Vemurafenib) Vem [MedChemExpress, MCE] orally twice daily at a dose of 50 mg/kg or (Anisomycin) ANS [MedChemExpress, MCE] once daily at a dose of 25 mg/kg, while Wedelolactone (Wed) [MedChemExpress, MCE] was intraperitoneally injected at a dose of 10 mg/kg. Assessments were made for body weight, rectal bleeding, and stool consistency, which were collectively used to compute disease activity index (DAI) scores [25]. Subsequently, after 7-day induction period, mice were anesthetized and euthanized. Colons were then harvested for subsequent analyses.

Histology Analysis

Tissue sections for histologic studies were immediately fixed in 4% buffered paraformaldehyde [Biosharp], followed by dehydration with ethanol and xylene, and embedded in paraffin. The paraffin-embedded tissues were sectioned at 5 μm for histological staining. H&E staining was performed using the H&E Staining Kit [LEAGENE], and Alcian Blue (AB) staining was conducted with the Alcian Blue Staining Kit [Beyotime], according to the manufacturer's protocols after deparaffinization. Histological scores for epithelial damage and inflammatory cell infiltration were conducted in a blinded manner, as previously reported [26]. Immunohistochemistry (IHC) staining was performed according to established protocols previously [27], with antibodies against TNF-α [1:200, Cell Signaling], IL-1β [1:200, Cell Signaling], IL-6 [1:200, Cell Signaling], F4/80 [1:200; Proteintech] and MPO [1:200, Proteintech], respectively.

For immunofluorescence (IF) analysis, the following antibodies were used: rabbit anti-ZAK [1:200, Proteintech], rabbit anti-Villin [1:200; Proteintech], rabbit anti-ZO1 [1:200, Aifang Biological], rabbit anti-Occludin [1:200, Proteintech] and rabbit anti-Muc2 [1:1000; Abcam]. Alexa Fluor 488 or 546 conjugated secondary antibodies (1:200) were used. Images were acquire using confocal fluorescence microscope [Zeiss LSM980 laser].

RNA Isolation and Quantitative Real-time PCR (qRT-PCR)

Total RNA was extracted using TRIzol reagent [Invitrogen, Thermo Fisher Scientific]. 1 μg of RNA was reverse transcribed into cDNA using the HiScript III RT SuperMix for qRT-PCR (+ gDNA wiper) kit [Vazyme]. PCR amplification was performed using the ChamQ SYBR qPCR Master Mix (High ROX Permixed) [Vazyme]. The qRT-PCR analysis was conducted using the Applied Biosystems StepOnePlus Real-Time PCR System [Thermo Fisher Scientific]. Each sample was tested in triplicate, and the experiment was independently repeated three times. The average Ct value of the reference gene (GAPDH) was subtracted from the average Ct value of the target gene. The relative fold change in mRNA expression was measured by using $2^{-\Delta\Delta Ct}$ method and normalized accordingly. The primer sequences were available in Supplementary Table 2.

Western Blot

Tissue and cell samples were lysed in RIPA buffer [Beyotime] containing protease inhibitor PMSF [Beyotime]. Protein extracts were separated by SDS-PAGE, transferred to PVDF membrane, and then incubated overnight at 4 °C with primary antibodies against ZA[1:3000; Proteintech], JNK [1:3000; Proteintech], p-JNK [1:2000; Cell Signaling Technology], p38 [1:3000; Proteintech], p-p38 [1:3000; Proteintech], ZO-1 [1:1000, Aifang Biological], Occludin [1:20,000; Proteintech], Caspase-1/Cleaved Caspase-1 [1:1000, Wanlei Biotechnology], Caspase-11 [1:1000; Abcam], GSDMD [1:1000; Abcam] or GAPDH [1:10,000, Proteintech]. Horseradish peroxidase (HRP)-linked secondary antibody [1:2000, Proteintech] was used. The HRP signal was visualized using 4200SF [Tanon]. Protein expression levels were quantified using ImageJ, and the results are presented as relative fold change and normalized accordingly.

Cell Culture

The mouse colon cell line C26 was purchased from ATCC [ATCC-1034], cultured in Dulbecco's Modified Eagle'sMedium (DMEM) [Hyclone] supplemented with penicillin–streptomycin (Gibco) and 10% heat inactivated fetal bovine serum (CellMax). The cells were incubated at 37 °C in humidified atmosphere with 5% CO2, and fresh medium was replenished every 2 or 3 days to maintain cell growth.

Propidium Iodide (PI)/Annexin-V Staining

After completing intervention, the cell culture medium was removed, and rinsed twice with PBS. Then Annexin-V/PI apoptosis reagent kit [SUNNCELL, Wuhan, China] was used for subsequent assays. After PI/Annexin-V solution incubation, the wells were rinsed 3 times with PBS. The cells were photographed under a microscope in dark environment.

siRNAs

Synthetic negative control [NC] siRNAs oligonucleotides [forward primer: UUCUCCGAACGUGUCACGUTT; reverse primer: ACGUGACACGUUCGGAGAATT] and mouse Caspase-11 siRNAs [forward primer: GGAUCAGAG AGUCUUCAAATT; reverse primer: UUUGAAGACUCU CUGAUCCTT] were synthesised by Hanbio Biotechnology Co.Ltd [Shanghai, China].

TUNEL Staining

After de-waxing, the 5 μm colon sections were immersed in 0.1 M citrate buffer (pH 6.0) and placed in a thermostat water bath at 95 ℃ for 15 min. Next, the sections were incubated with TUNEL reaction mixture [Aifang Biological] for 1 h at 37 °C. The nuclei were counterstained with DAPI. Staining images were captured under a confocal fluorescence microscope [Zeiss LSM980 laser] at 400 × magnification. For each mouse, 3 to 5 random fields of the colon were captured per section.

ELISA

Colonic tissues were homogenized to extract the supernatant for cytokine analysis. ELISA kits were used to measure the levels of TNF-α, IL-1β, and IL-6 (all from Aifang Biological) in supernatant. The absorbance of the samples was measured at 450 nm using a microplate spectrometer [Varioskan LUX Multifunctional Enzyme Labeler (Microplate Assay)].

Statistical Analysis

Continuous data were presented as Mean ± SEM or Mean ± SD, and the categorical variables were reported as frequency and percentage. Data were analyzed using Graphpad Prism 9 software. Data comparison between two groups was performed using the *t*-test for normally distributed data, otherwise, the Mann–Whitney test was used. For comparisons among multiple groups, one-way analysis of variance (ANOVA) was used. Correlation analysis was performed to assess relationships between variables. A p-value < 0.05 was considered as statistically significant.

Results

A Higher ZAKα Expression in Colonic Epithelium of UC Patients and Mouse Models of Colitis

Firstly, we sought to investigate the expression level of the key driving protein ZAKα of RSR in UC colon. IF staining was performed using Villin (an intestinal epithelial marker) and ZAK antibodies. The IF analysis showed that Villin expression did not exhibit significant changes between the UC and control groups; however, a marked increase in ZAK expression was observed in the UC colonic epithelium (Fig. 1A). The expression level of ZAKα protein and mRNA were further confirmed by qRT-PCR and Western blot analysis (Fig. 1B, E and F). Moreover, a larger RNA-seq dataset (335 controls *vs* 680 UC samples) was selected from GEO database to validate the level of ZAK expression, and the results showed a significant increase in ZAK expression in colonic biopsies of UC patients compared to controls (Fig. 1C). Furthermore, ZAK expression was significantly higher in inflamed colonic tissues compared to non-inflamed colonic tissues in UC patients (Figure S1A). Meanwhile, we aimed to evaluate the impact of different biologics on ZAK expression in UC patients using the GEO database. The results indicated that treatment with Vedolizumab, Ustekinumab, and Tofacitinib had no significant effect on ZAK expression in colonic tissues of UC patients (Figure S1C, D and E). Notable, the expression of ZAK in the colonic tissue appears to be reduced after Infliximab treatment (Figure S1B). ZAKα is a key protein in ZAKα-driven RSR, prompting us to investigate whether the downstream pathways of RSR are activated in the colonic tissues of UC patients. We assessed the phosphorylation status of key downstream molecules, p38 and JNK. The results showed that the phosphorylation levels of JNK and p38 were significantly elevated in the colonic tissues of UC patients compared to the control group (Fig. 1E, F).

Subsequently, we examined the expression of ZAKα in colonic tissues of DSS-induced mice model of colitis. Similarly, IF demonstrated high ZAK expression in colitis group (Fig. 1C), which was confirmed by Western blot analysis (Fig. 1G, H). Then, we assessed the phosphorylation status of p38 and JNK, and the results indicated that the phosphorylation levels of JNK and p38 were significantly increased in the colonic tissues of DSS-induced colitis mice compared to the control group (Fig. 1G, H).

To elucidate whether ZAKα expression was related to disease activity, we conducted correlation analyses. The

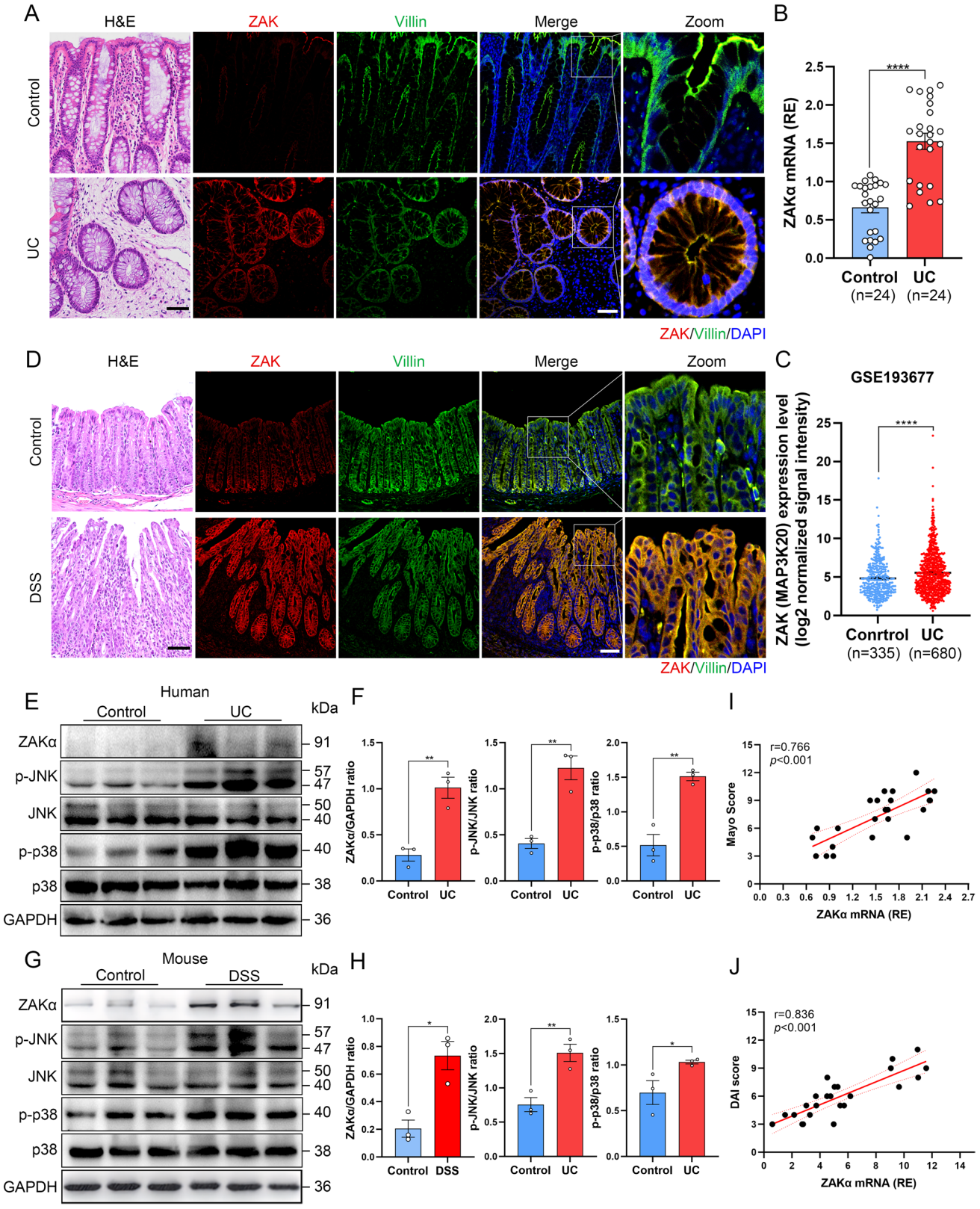

results indicated a positive correlation between ZAKα mRNA expression levels and Mayo scores in UC patients (Fig. 1I). Likewise, in the DSS colitis mice, ZAKα mRNA levels exhibited a significant correlation with the Disease Activity Index (DAI) scores (Fig. 1J).

◂**Fig. 1** ZAKα expression in colonic epithelial cells of UC patients and DSS-induced colitis models. **A** Immunofluorescence staining of human colonic tissues. ZAKα (red), Villin (green; an intestinal epithelial cell marker), DAPI (blue). Scale bar = 50 μm; **B** qRT-PCR detection of ZAKα expression in control and UC patient colonic tissues. Control group (n = 24), UC group (n = 24); **C** The ZAK expression level from RNA-seq performed in colonic biopsies of healthy controls (n = 335) and UC patients (n = 680) from GEO datasets (GSE193677); **D** Immunofluorescence staining of colonic tissues from DSS-induced colitis mouse model. ZAKα (red), Villin (green; an intestinal epithelial cell marker), DAPI (blue). Scale bar = 50 μm; **E, F** Western blot detection and quantification analysis of ZAKα, p-JNK, JNK, p-p38 and p38 protein levels in control and UC patient colonic tissues; **G, H** Western blot detection and quantification analysis of ZAKα, p-JNK, JNK, p-p38 and p38 protein levels in colonic tissues of control and DSS-induced colitis model mice; **I** Correlation analysis between ZAKα mRNA expression in human colonic tissues and Mayo scores. Control (n = 24), UC group (n = 24); **J** Correlation analysis between ZAKα mRNA expression in mouse colonic tissues and Disease Activity Index (DAI). Control group (n = 24), DSS group (n = 24). Data were analyzed using two-tailed unpaired t-tests for normal distribution, otherwise, Mann–Whitney test was used, and presented as Mean ± SEM. Correlation analysis was performed to assess relationships between variables. Representative data from at least 3 independent experiments are shown. * p < 0.05, *** p < 0.001

ZAKα Inhibition Alleviated DSS-induced Colitis in Mice

To elucidate whether ZAKα is involved in the pathogenesis of colitis, we induced acute colitis in mice by DSS, concurrently administering either ZAK inhibitor (Vemurafenib, Vem) [28] or RSR activator (Anisomycin, ANS) [29]. The specific dosing regimen was outlined in Fig. 2A. Compared to DSS alone mice, those receiving Vem showed significantly less weight loss (Fig. 2B) and decreased shortening of colon (Fig. 2C, E). In contrast, ANS exacerbated DSS-induced colitis (Fig. 2 B-E). Histological analysis revealed that, mice treated with Vem exhibited reduced colonic epithelial damage, limited inflammatory cell infiltration, and lower histological scores, whereas mice in ANS group showed the opposite (Fig. 2F, G).

Inhibition of ZAKα Alleviated Inflammatory Response in DSS-colitis Mice

Next, we aimed to investigate the effects of ZAKα inhibition on inflammatory cytokines and immune cell infiltration. DSS induced mRNA expression of various pro-inflammatory cytokines in colonic mucosa, including TNF-α, IL-1β, IL-6, INF-γ, CCL-5, CXCL-16, and Hmgb-1, while the expression of anti-inflammatory cytokine IL-10 was markedly suppressed (Fig. 3 A-H). However, following treatment with Vem, these pro-inflammatory cytokines were significantly decreased, while the anti-inflammatory cytokines notably increased.

Notably, mice treated with ANS exhibited increased mRNA expression of colonic pro-inflammatory cytokines and decreased anti-inflammatory cytokines (Fig. 3A-H). Furthermore, we performed IHC analysis to further examine the expression of pro-inflammatory factors (TNF-α, IL-1β, and IL-6), and the observed trends were consistent with the mRNA expression (Fig. 3I). IHC staining for myeloperoxidase (MPO) and F4/80 demonstrated that Vem treatment restricted the mucosal infiltration of neutrophils and macrophages induced by DSS (Fig. 3J-M). Conversely, ANS treatment exacerbated the infiltration of these two cell types (Fig. 3J-M).

Inhibition of ZAKα Ameliorates Mucosal Barrier Disruption in DSS-colitis Mice

Then, we examined the impact of ZAKα on mucosal barrier in DSS-colitis mice. Compared to control group, expression of tight junction proteins ZO-1 and Occludin were significantly increased in Vem group and decreased in ANS mice (Fig. 4A, B). Western blot analysis further confirmed the above results (Fig. 4C, D). Alcian blue staining revealed that additional Vem therapy exhibited reduced loss of goblet cells, whereas ANS treatment showed increased loss (Fig. 4E, F), IFC staining of $Muc2^+$ cells revealed similar results (Fig. 4G, H).

ZAKα Activation Induced Pyroptosis Via the Non-canonical Pathway Involving Caspase-11/GSDMD In Vitro

Previous studies indicated that ZAKα can induced pyroptosis in human keratinocytes via NLRP1 inflammasome pathway [21, 30], however, the murine cell lacks the connecting region containing both ZAKα and the p38 phosphorylation site of NLRP1 [22]. Additionally, activation of RSR can lead to various forms of cell death including apoptosis [22]. Firstly, we treated mouse colonic cell line C26 with 10 μM ANS, and after 5 h, stained with PI and Annexin V. The results showed a significant increase in PI^+ cells in the C26 cell line after ANS treatment (Fig. 5A, B), while the number of Annexin-V-positive cells showed no significant difference (Fig. 5A). This suggested that ZAKα activation can induce pyroptosis rather than apoptosis in mouse colonic cells.

Since pyroptosis primarily proceeds via the canonical pathway involving inflammasome-Caspase-1 or the non-canonical pathway involving Caspase-11 [31], we examined the levels of total and cleaved forms of Caspase-1, Caspase-11, and GSDMD in cell lysates using Western blot analysis. ANS treatment led to a significant reduction in total Caspase-11 and GSDMD, accompanied by marked increase in cleaved active forms. However, there were no significant changes in total or cleaved Caspase-1 (Fig. 5C, D).

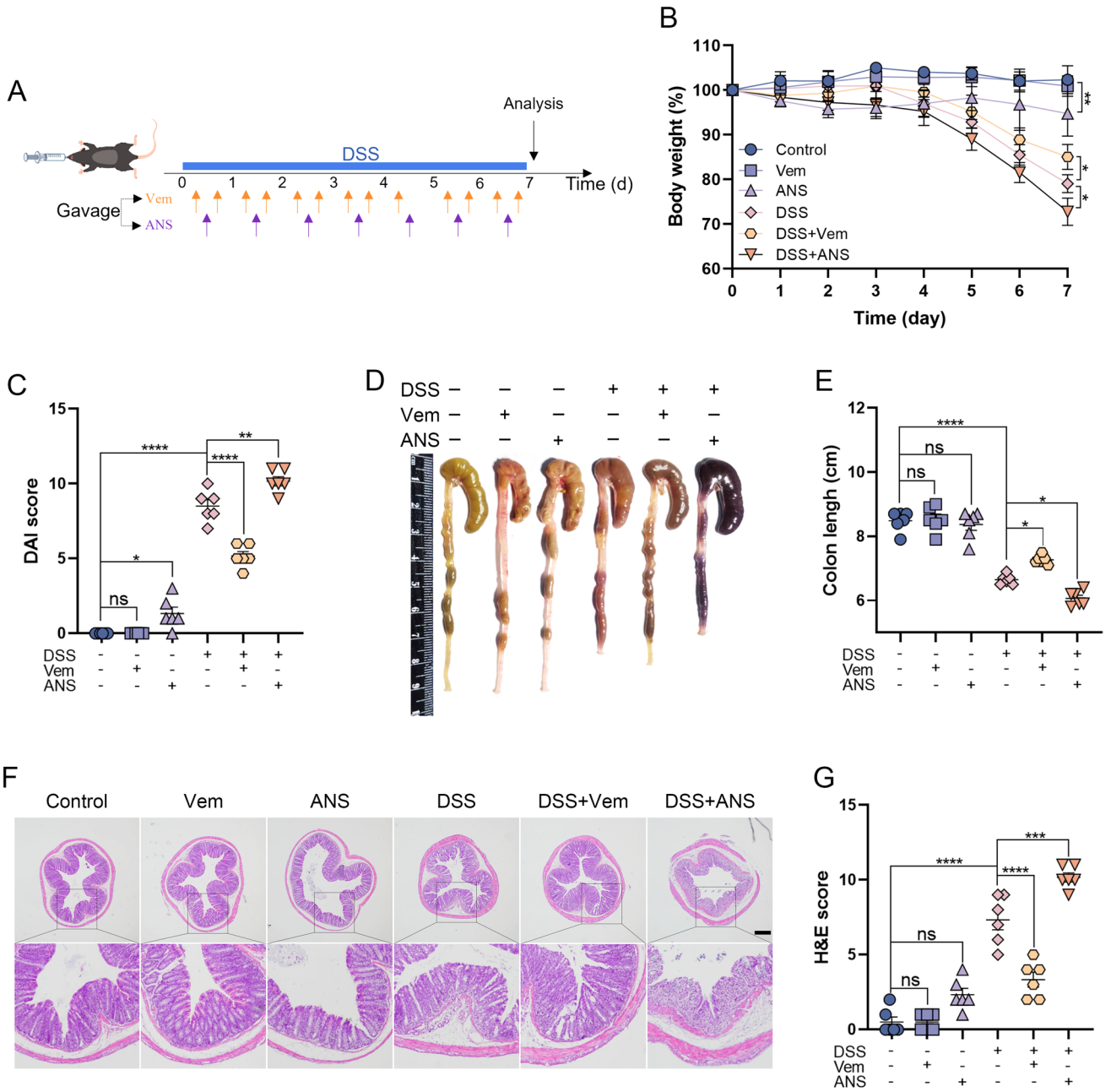

Fig. 2 Inhibition of ZAKα attenuates DSS-induced colitis. **A** Schematic representation of the mouse dosing regimen, outlining the experimental setup for DSS-induced colitis model experimentation and collection of colonic samples. Female mice were administered 2.5% DSS in drinking water for 7 days, during which Vem was administered via oral gavage twice daily at a dose of 50 mg/kg each time, while ANS was administered once daily at a dose of 25 mg/kg each time, with each group consisting of six mice ($n = 6$). Colonic samples were collected on day 7; **B, C** Monitoring of daily changes in mouse body weight during the experimental period and DAI score on the final day; **D, E** Isolation of colonic tissues on the final day of the experiment, providing representative images of colonic tissues from each group, and recording of colonic lengths; **F, G** H&E staining of mouse colonic tissues and histological analysis. Scale bar = 100 μm. Data were analyzed using one-way ANOVA and presented as Mean ± SEM, with representative data from at least three independent experiments, * $p < 0.05$, ** $p < 0.01$, *** $p < 0.001$, **** $p < 0.0001$

Moreover, we aimed to further elucidate whether Caspase-11 is involved in ZAKα induces pyroptosis. We employed siRNA-mediated knockdown of Caspase-11 in C26 cell line, followed by treatment with ANS. PI staining revealed that, upon Caspase-11 knockdown, the number of PI-positive cells significantly decreased after

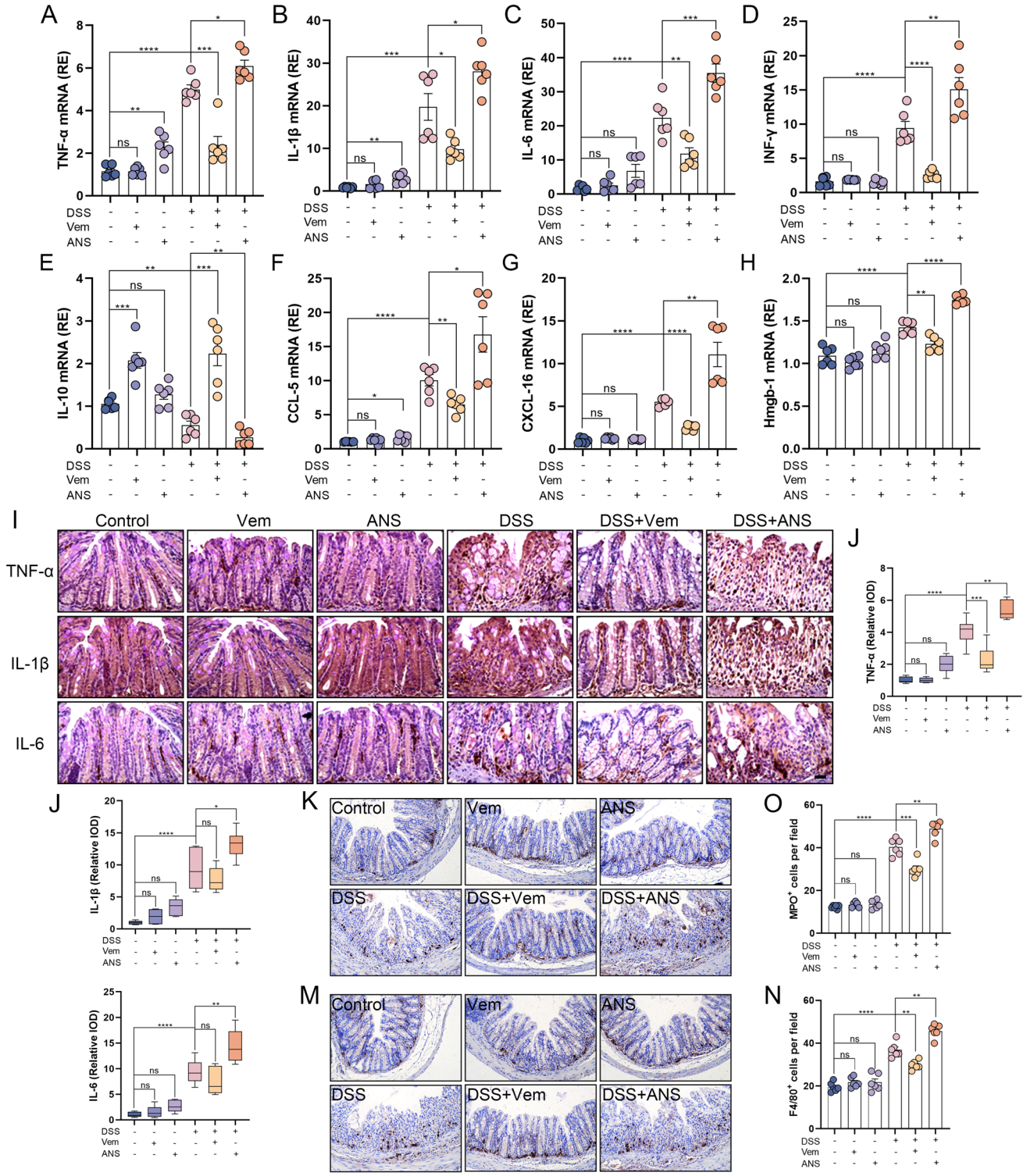

Fig. 3 Inhibition of ZAKα attenuates the expression of pro-inflammatory cytokines and immune cell infiltration in DSS-induced colitis. **A-H** qRT-PCR analysis of the expression of inflammatory factors in colonic tissues from each group. Each group (n = 6); **I, J** Immunohistochemical detection of TNF-α, IL-1β, and IL-6 in colonic tissues from each group of mice, and the staining intensity was quantitatively analyzed, Scale bar = 25 μm; **K, O** Immunohistochemical detection of MPO expression in colonic tissues from each group of mice and quantification of MPO^+ cells, Scale bar = 50 μm; **M, N** Immunohistochemical detection of F4/80 expression in colonic tissues from each group of mice and quantification of $F4/80^+$ cells, Scale bar = 50 μm, each group (n = 6). Data were analyzed using one-way ANOVA and represented as Mean ± SEM, with data representative of at least three independent experiments, * p < 0.05, ** p < 0.01, *** p < 0.001, **** p < 0.0001

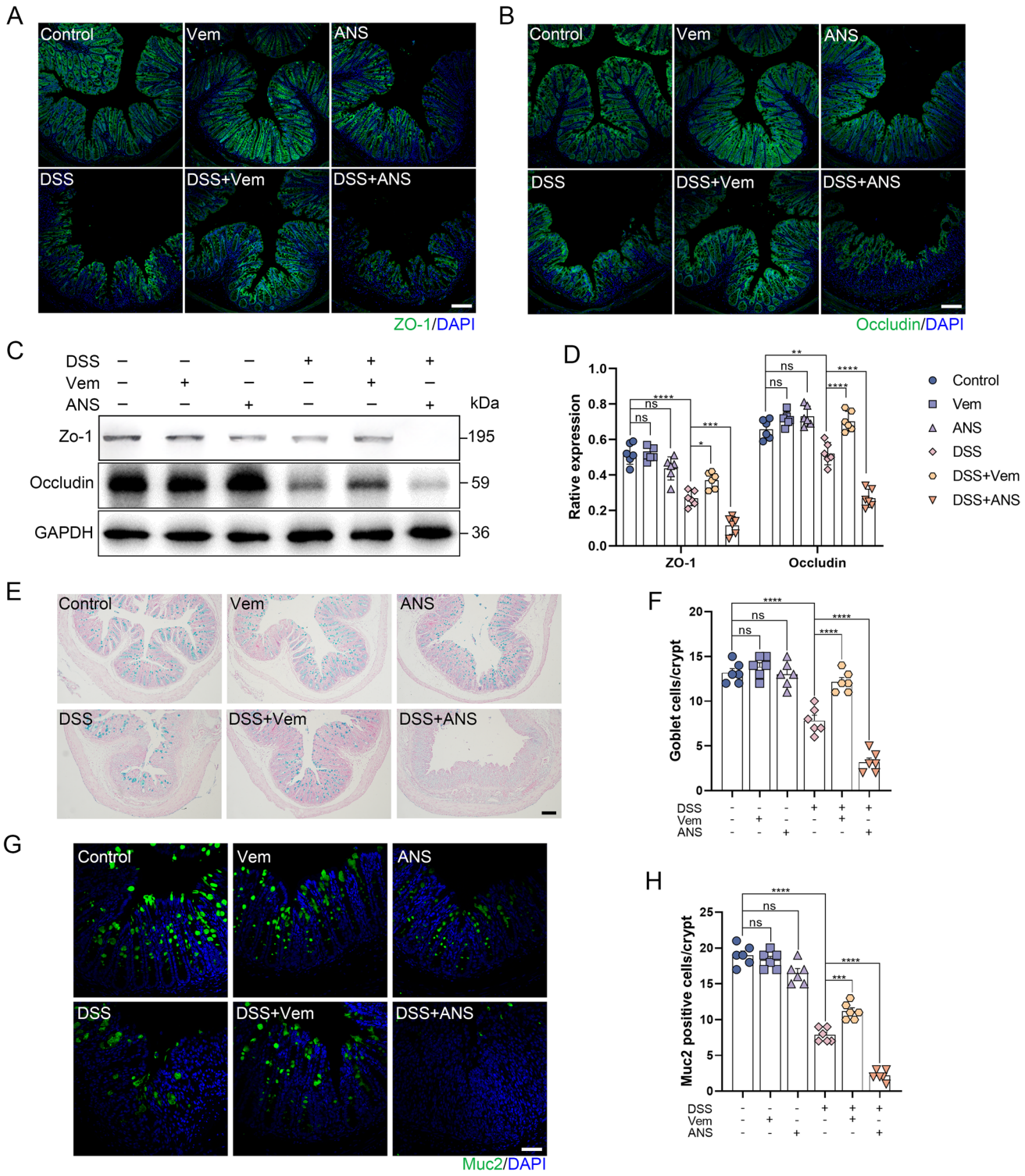

Fig. 4 Inhibiting ZAKα can ameliorate colonic barrier damage in the DSS-induced colitis model. **A, B** Immunofluorescence staining was performed on the last day of the experiment to determine the localization of ZO-1 and Occludin in mouse colons, Scale bar = 100 μm; **C, D** Western blot analysis was conducted to measure the expression levels of ZO-1 and Occludin in mouse colons and quantitatively analyze the results; **E, F** Histological analysis and goblet cell counting in mouse colonic tissues were performed using Alcian blue staining; **G, H** Immunofluorescence staining was utilized to assess the localization of Muc2 in mouse colons and to quantify the number of $Muc2^{+}$ cells, Scale bar = 50 μm. Data were analyzed using one-way ANOVA and expressed as Mean ± SEM, with representative results from at least 3 independent experiments, * $p < 0.05$, ** $p < 0.01$, *** $p < 0.001$, **** $p < 0.0001$

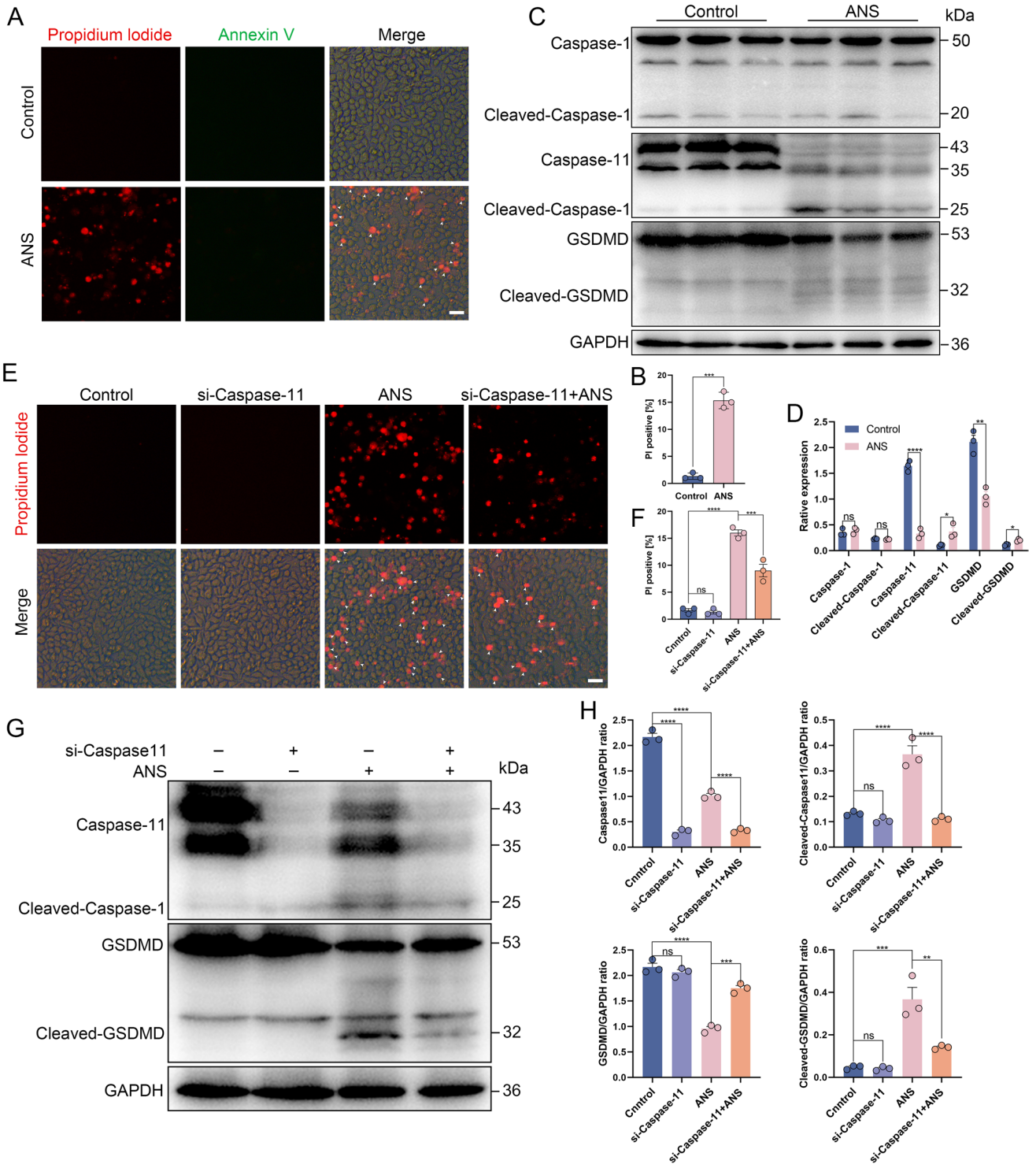

Fig. 5 Activation of ZAKα induces caspase-11-mediated pyroptosis. **A, B** Mouse colonic cells C26 treated with 10 μM ANS for 5 h were stained with Propidium Iodide (PI) and Annexin-V, and the number of PI^+cells was quantified. Scale bar = 25 μm; **C, D** Western blot analysis of total protein levels and cleaved forms of Caspase-1, Caspase-11, and GSDMD in C26 cells treated with 10 μM ANS for 5 h, with quantification; **E, F** PI staining to detect PI + cells in C26 cells treated with ANS or siRNA-Caspase-11, with quantification. Scale bar = 25 μm; **G, H** Western blot analysis of total protein levels and cleaved forms of Caspase-11 and GSDMD in C26 cells treated with 10 μM ANS for 5 h, with or without siRNA-Caspase-11, with quantification. Data were analyzed using one-way ANOVA and are presented as Mean ± SEM, with representative data from at least 3 independent experiments, * $p < 0.05$, ** $p < 0.01$, *** $p < 0.001$, **** $p < 0.0001$

ANS treatment (Fig. 5E, F). Western blot analysis further confirmed that, upon Caspase-11 knockdown, the cleaved, active form of GSDMD decreased after ANS treatment (Fig. 5G, H). These findings suggested that ZAKα, at least in part, induces pyroptosis via Caspase-11/GSDMD.

Inhibition of ZAKα Reduces DSS-induced Colonic Epithelial Cell Pyroptosis in Mice

Then, we aimed to investigate whether ZAKα can trigger pyroptosis through Caspase-11/GSDMD pathway in *vivo*. In Vem treated DSS mice, there was a significant reduction in cleaved forms of Caspase-11 and GSDMD (Fig. 6 A, B).

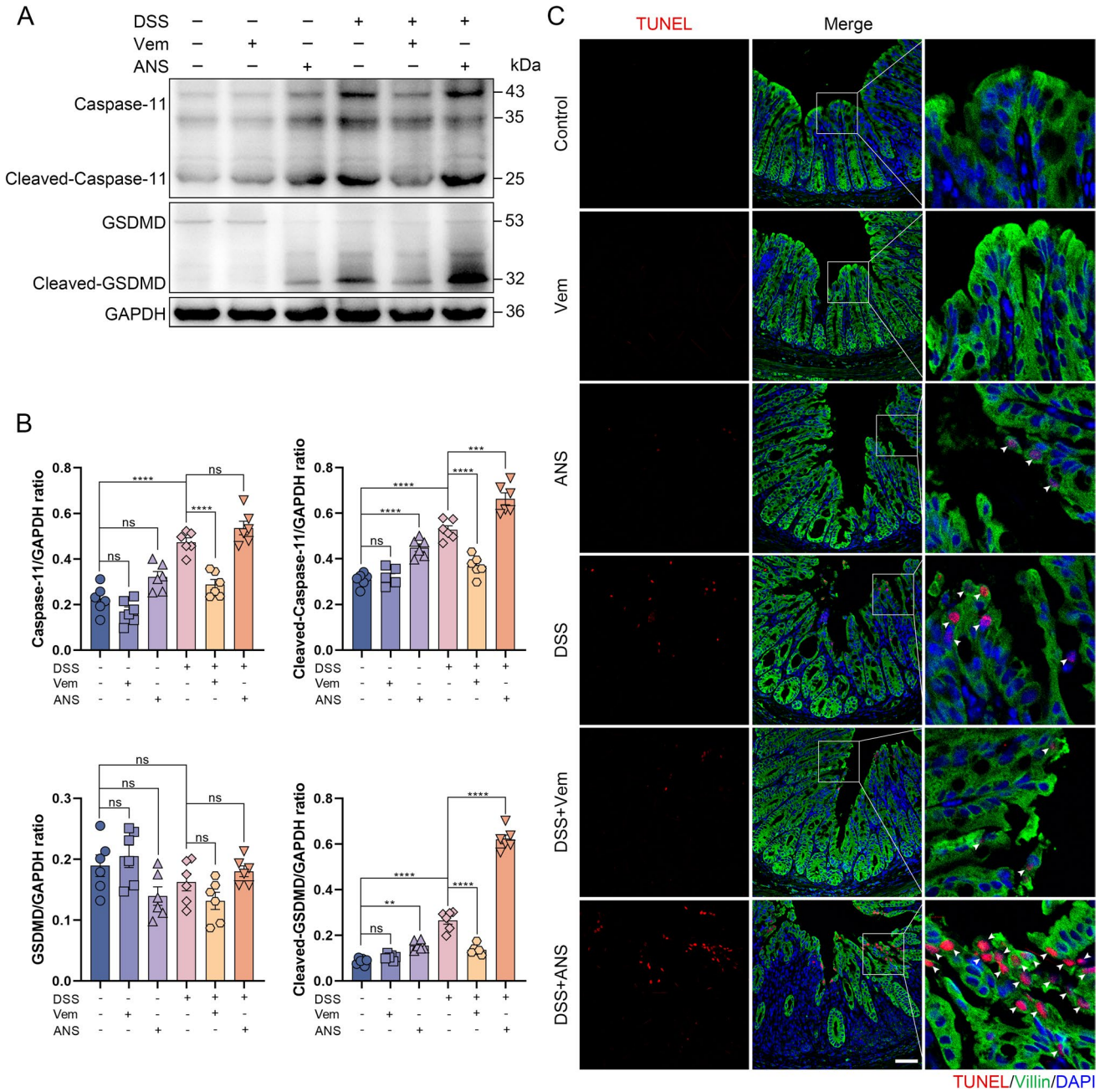

Fig. 6 Inhibition of ZAKα reduces intestinal epithelial pyroptosis in DSS-induced colitis mice. **A, B** Western blot analysis was employed to detect the total protein levels of Caspase-11 and GSDMD in each group of mice, as well as their respective cleaved forms, with statistical quantification performed; each group ($n = 6$); **C** TUNEL staining was conducted on mouse colons in each group, with TUNEL (red), Villin (green), and DAPI (blue) staining shown; Scale bar = 50 μm. Data were analyzed using one-way ANOVA and expressed as Mean ± SEM, with representative results from at least 3 independent experiments, ** $p < 0.01$, *** $p < 0.001$, **** $p < 0.0001$

Conversely, treatment with ANS significantly increased both (Fig. 6A, B). It is noteworthy that ANS alone also led to an increase in the cleaved forms of Caspase-11 and GSDMD in mice (Fig. 6 A, B). Additionally, since the late stage of pyroptosis can render cells positive for TUNEL staining [32], we performed TUNEL and Villin co-staining from each group of mice. Vem treatment reduced the number of TUNEL-positive cells induced by DSS, while ANS treatment exacerbated this phenomenon (Fig. 6C).

Inhibitors of Caspase-11 Alleviated the Exacerbation of Colitis Induced by ZAKα Activation in Colitis Models

Finally, we aimed to investigate whether inhibition of Caspase-11 could alleviate the exacerbation of DSS-induced colitis in mice triggered by ZAKα activation. Mice were treated with 2.5% DSS to induce acute colitis, with or without the use of a Caspase-11 inhibitor (Wedelolactone, Wed) [33] and ANS during this process (Fig. 7A). Compared to ANS treated DSS-colitis mice, additional administration of Wed resulted in a significant reduction in body weight loss (Fig. 7B), DAI scores (Fig. 7C), and shortening of colonic length (Fig. 7D, E). H&E staining results revealed that colonic crypt loss was reduced in mice treated with Wed, accompanied by lower histological scores (Fig. 7F, G).

The expression of inflammatory cytokines were also evaluated. Wed significantly reduced the mRNA expression of the inflammatory cytokines TNF-α, IL-1β, and IL-6 in ANS-treated DSS-colitis mice (Fig. 7H). This phenomenon was further confirmed by ELISA analysis (Fig. 7I). In summary, our experimental findings suggest that inhibition of Caspase-11 attenuates the exacerbation of DSS-induced colitis mediated by ZAKα activation.

Discussion

The traditional perspective suggested that ribosomal translation impairments on mRNA are presumed to result in mRNA and nascent protein degradation [34, 35]. However, recent investigations indicated that ribosomal stalling and collisions can actually serve as pivotal signaling hubs, recruiting diverse participants to activate specific pathways based on the "severity" of the damage, ultimately determining cell fate [16, 17]. One significant pathway among these is the ZAKα-driven RSR (ribosome-associated signaling response) [11]. This study revealed that the key protein kinase ZAKα, orchestrating RSR, exhibits increased expression in colonic epithelium of UC patients and DSS colitis mouse models. Moreover, inhibiting ZAKα alleviated DSS-induced colitis. Activation of RSR consequently induced pyroptosis in mouse colonic epithelial cells via the Caspase-11/GSDMD non-canonical pathway.

Consistent with our findings, several studies have highlighted the role of ZAKα-driven RSR in triggering inflammatory responses. For instance, ultraviolet radiation can activate RSR leading to the activation of NLRP1 inflammasomes, or RSR can indirectly activate NLRP1 inflammasomes via p38 activation, resulting in pyroptosis of human keratinocytes and the subsequent releasing of mature IL-1β and IL-18, thereby initiating inflammatory reactions [21]. Meanwhile, reactive oxygen species (ROS) are recognized as pivotal factors in initiating inflammatory processes. Mitochondrial ROS, for example, can impede TFAM-mediated maintenance of mitochondrial DNA, resulting in diminished mitochondrial energy metabolism and subsequent inflammation [36]. Excessive ROS production is also implicated in UC, exacerbating its onset and progression through oxidative damage to DNA, proteins, and lipids [37]. Recent studies have indicated that ROS can trigger ribosomal damage and activate ZAKα [18], suggesting that ROS-induced colitis might be mediated through the ZAKα-driven RSR pathway, necessitating further investigation.

Other relevant evidences indicate that ZAKα-driven RSR can directly phosphorylate and activate p38 and JNK, both of which are closely linked to colitis. Galia et al. developed inhibitors targeting the binding regions of p38 and JNK to their input proteins. These inhibitors disrupt the interaction between p38 and JNK with input proteins, hampering their nuclear translocation and subsequent phosphorylation of nuclear substrates. Administering these inhibitors effectively attenuates inflammation in mice [38]. Furthermore, a study focusing on p38 revealed that a high-salt diet can exacerbate colitis in a mouse model through the p38/MAPK signaling pathway [39]. Additionally, Stanniocalcin-1 (STC1) can interact with PARP1 to activate the JNK pathway, thereby increasing the susceptibility of mice to DSS-induced colitis. Inhibiting JNK can alleviate parthanatos and inflammatory damage induced by STC1 overexpression [40]. The aforementioned evidence suggests that activation of p38 and JNK by ZAKα-driven RSR may exacerbate colitis, which is consistent with our experimental findings.

Certainly, the non-canonical pyroptosis pathway also plays a crucial role in UC. In a study concerning the oxidative stress sensor GPx8, researchers observed that cysteine 79 of GPx8 forms a disulfide bond with cysteine 118 of Caspase-4, thereby covalently inhibiting the activation of Caspase-4/11. Deficiency of GPx8 leads to Caspase-4/11-induced colitis and septic shock inflammatory responses [5]. Additionally, small molecule inhibition of Caspase-4/11 activation can reduce the severity of colitis in GPx8 knockout mice [5]. Interestingly, in colonic tissues of UC patients, the expression levels of GPx8 are low, while the expression levels of Caspase-4 are high [5]. Moreover, it has been found

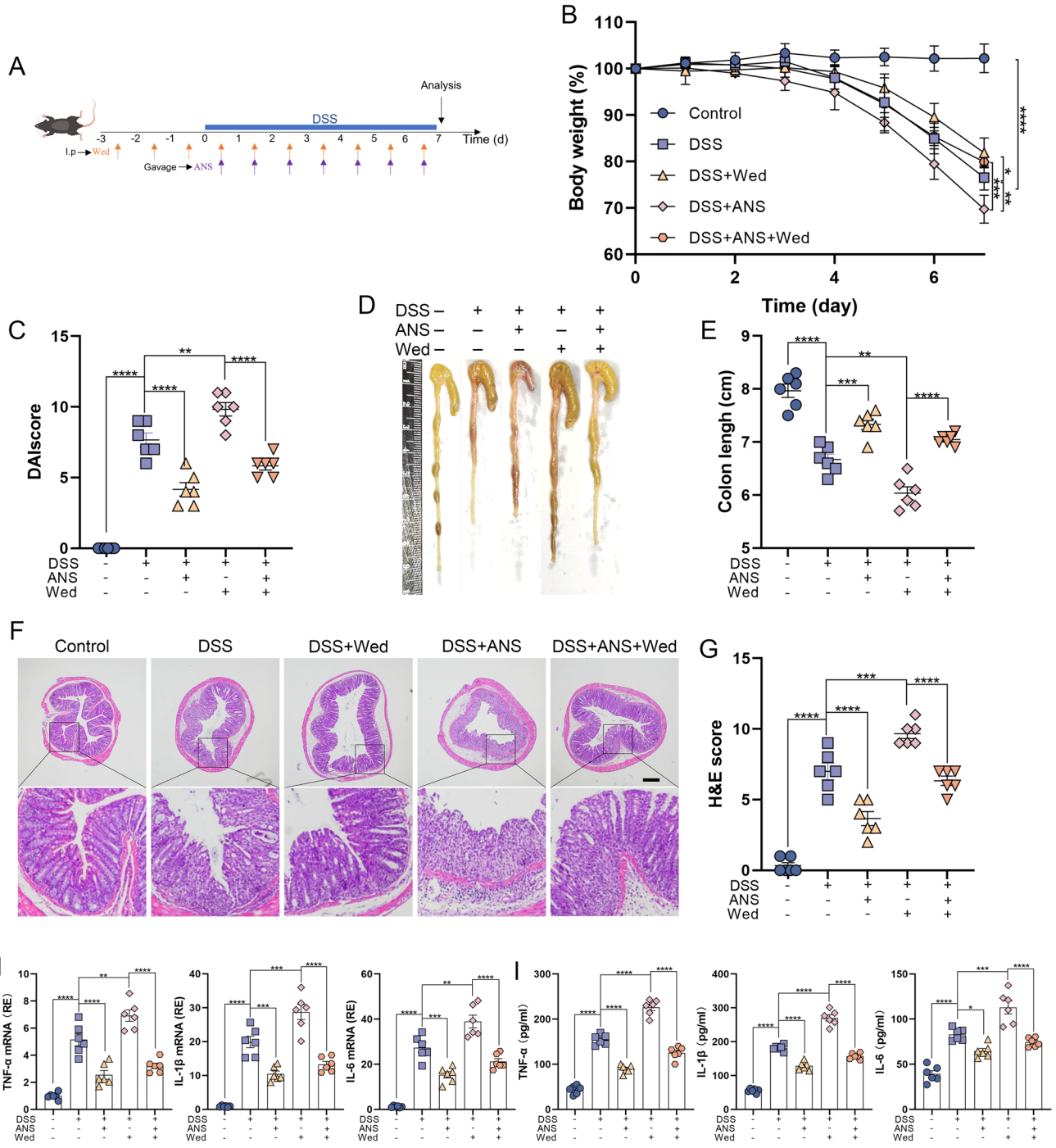

Fig. 7 Inhibition of Caspase-11 alleviates exacerbation of colitis induced by ZAKα activation. **A** Schematic representation of the mouse administration protocol, detailing the experimental setup for inducing DSS-induced colitis and collecting colonic samples. Female mice were provided with drinking water containing 2.5% DSS for 7 days, with Wed administered via intraperitoneal injection at 10 mg/kg/day for 3 days prior to DSS treatment and continued until the end of the experiment, and ANS administered via daily oral gavage at 25 mg/kg/day starting from DSS treatment until the end of the experiment, with each group consisting of 6 mice ($n = 6$). Colonic and blood samples were collected on day 7; **B, C** Monitoring of daily changes in mouse body weight throughout the experiment and the DAI score on the final day; **D, E** On the final day of the experiment, colonic tissues were isolated, representative photographs of colonic tissues from each group were provided, and colonic length was recorded; **F, G** H&E staining of mouse colonic tissues and histological analysis. Scale bar = 250 μm. **H** qRT-PCR analysis of the expression of inflammatory cytokines (TNF-α, IL-1β, and IL-6) in colonic tissues from each group ($n = 6$); **I** ELISA detection of TNF-α, IL-1β, and IL-6 expression in colonic tissues of each group of mice. Data are presented as Mean ± SEM and were analyzed using one-way ANOVA, with at least three independent experiments represented, * $p < 0.05$, ** $p < 0.01$, *** $p < 0.001$, **** $p < 0.0001$

that *pneumonia Klebsiella pneumoniae* (KLP) exacerbates colitis and is closely associated with Caspase-11 activation. Further investigation revealed that KLP's lipopolysaccharide can bind to Caspase-11, activating it and inducing mature IL18 in mouse and human colonic organoids [41]. Another study found that human umbilical cord mesenchymal stem cell-secreted exosomes (hucMSC-Ex) containing miR-203a-3p.2 inhibit Caspase-11 activation, reduce the secretion of interleukin (IL)−1β, IL-6, and Caspase-11, thereby alleviating macrophage pyroptosis and reducing colitis in mice [42]. It is noteworthy that several studies suggest a protective role for Caspase-11 in colitis. For instance, Katarzyna et al. demonstrated in experiments with Caspase-11 knockout mice that the increased susceptibility of Caspase-11-deficient mice to DSS-induced colitis is attributed to impaired IL-18 generation, leading to reduced proliferation and increased cell death of intestinal epithelial cells [43]. Further experiments in hematopoietic and non-hematopoietic cells revealed that the gene expression and function of Caspase-11 contribute to alleviating DSS-induced colitis in mice [44]. Despite standardizing the microbiota among experimental groups of mice, Caspase-11 knockout mice still exacerbated DSS-induced colitis [45]. Additionally, a study suggest that Caspase-11 can reduce pro-inflammatory *Prevotella* and shape the composition of the gut microbiota to resist colitis [46]. However, the latest relevant research indicated that Caspase-11 does not affect chronic experimental colitis, and its role in acute DSS colitis varies depending on environmental factors including the microbiota, particularly the presence of clostridial spores [47].

In our study, we did not investigate the factors that activate ZAKα-driven RSR to exacerbate colitis. However, several studies have suggested that microbial factors can induce ZAKα-driven RSR. For example, Dakshina et al. demonstrated that Shiga toxins (Stxs) from Escherichia coli can cleave a single adenine residue on the alpha-sarcin loop of the 28S ribosomal RNA, activating ZAK-driven RSR [13, 48]. Diphtheria toxin produced by the human diphtheria pathogen can trigger ZAK-driven RSR, leading to NLRP1 phosphorylation and inducing pyroptosis in human keratinocytes [22]. Additionally, mycotoxins such as Anisomycin and Deoxynivalenol are known RSR agonists [11, 21]. Given the close relationship between gut microbes and UC, it is plausible that the activation of ZAKα-driven RSR in the colonic tissues of UC patients is linked to gut microbiota. Moreover, ZAK appears to play a significant role in immune cells. For instance, Yan et al. found that the KU complex recognizes accumulated cytoplasmic DNA in aged human and mouse $CD4^+$ T cells, which facilitates the recruitment of DNA-PKcs and phosphorylation of the kinase ZAK, ultimately promoting $CD4^+$ T cell proliferation and activation [49]. However, our study primarily focuses on the role of ZAKα and its driven RSR in the colonic epithelium in the pathogenesis of UC, though the involvement of ZAKα-driven RSR in immune cells presents an intriguing avenue for further research on the onset and progression of UC.

In this study, the following limitations were identified: Firstly, since the activation of the RSR is driven by collisions or stalling of ribosomes on mRNA, leading to activation of ZAKα, we did not perform specific assays for ribosome stalling or collisions. Instead, we only examined the expression of ZAKα, thus lacking direct evidence of ribosome stalling or collisions; Secondly, we found that the control group was significantly older than the UC group in our included population. However, the effect of age on ZAKα has not been explored in depth, and this would be worth investigating in future studies. Thirdly, the inhibitor used in this study, including Vemurafenib and Wedelolactone, are not specific inhibitors, may have relatively weak efficacy. Further validation using ZAKα and Caspase-11 knockout mice are necessary to confirm our study results; Fourthly, RSR activation can induce various cellular effects. In our assessment of RSR activation's influence on cell death pathways, we only examined a single indicator for pyroptosis and apoptosis. Other relevant indicators were not assessed, and other cell death pathways were overlooked; Fifthly, when detecting epithelial pyroptosis in the mouse colon through Western blot analysis, we extracted total colon proteins for analysis without isolating epithelial cells or crypts for examination. Sixthly, we utilized only a DSS-induced colitis mouse model, which should be further validated using other models, such as TNBS-induced or IL-10 knockout mouse models.

In all, UC is a complex, multifactorial disease that likely involves multiple signaling pathways and mechanisms. However, the ZAKα seems to play a significant role in the pathogenesis of UC, potentially triggering pyroptosis in colonic epithelial cells in part via the Caspase11/GSDMD pathway. Of note, our study established, for the first time, a mechanistic link between ribosomal translational impairment mediated by ZAKα and the pathogenesis of UC. Meanwhile, we observed that the administration of a specific structural inhibitor targeting ZAKα could ameliorate DSS-induced colitis in mice, thus presenting a promising avenue for the clinical management of UC and underscoring the need for further investigations in this direction.

Supplementary Information The online version contains supplementary material available at https://doi.org/10.1007/s10753-025-02262-z.

Acknowledgements This work was supported by grants from the National Natural Science Foundation of China, Grant/Award Number: 81970469.

Author Contributions SL, MC, WA, WZ, YG and ZY performed the expriments and data collection. SL, MC, SZ, FZ, ZY, LZ, CD and JG provided clinical samples, protocols, reagents, or designed

experiments. SL, MC, WA and JG analysed and interpreted the data, and drafted the manuscript. All authors critically revised the manuscript for important intellectual content.

Funding This work was supported by grants from the National Natural Science Foundation of China, Grant/Award Number: 81970469.

Data Availability No datasets were generated or analysed during the current study.

Declarations

Competing Interests The authors declare no competing interests.

References

1. Le Berre, C., S. Honap, and L. Peyrin-Biroulet. 2023. Ulcerative colitis. *Lancet* 402 (10401): 571–584.
2. Frank, D., and J. E. Vince. 2019. Pyroptosis versus necroptosis: Similarities, differences, and crosstalk. *Cell Death and Differentiation* 26 (1): 99–114.
3. Hadian, K., and B. R. Stockwell. 2023. The therapeutic potential of targeting regulated non-apoptotic cell death. *Nature Reviews Drug Discovery* 22 (9): 723–742.
4. Bulek, K., J. Zhao, Y. Liao, et al. 2020. Epithelial-derived gasdermin D mediates nonlytic IL-1beta release during experimental colitis. *The Journal of Clinical Investigation* 130 (8): 4218–4234.
5. Hsu, J. L., J. W. Chou, T. F. Chen, et al. 2020. Glutathione peroxidase 8 negatively regulates caspase-4/11 to protect against colitis. *EMBO Molecular Medicine* 12 (1): e9386.
6. Yang, W., Y. Wang, T. Wang, et al. 2023. Protective effects of IRG1/itaconate on acute colitis through the inhibition of gasdermins-mediated pyroptosis and inflammation response. *Genes & Diseases* 10 (4): 1552–1563.
7. An, Y., Z. Zhai, X. Wang, et al. 2023. Targeting Desulfovibrio vulgaris flagellin-induced NAIP/NLRC4 inflammasome activation in macrophages attenuates ulcerative colitis. *Journal of Advanced Research* 52: 219–232.
8. Iordanov, M. S., D. Pribnow, J. L. Magun, et al. 1997. Ribotoxic stress response: Activation of the stress-activated protein kinase JNK1 by inhibitors of the peptidyl transferase reaction and by sequence-specific RNA damage to the alpha-sarcin/ricin loop in the 28S rRNA. *Molecular and Cellular Biology* 17 (6): 3373–3381.
9. Gross, E. A., M. G. Callow, L. Waldbaum, et al. 2002. MRK, a mixed lineage kinase-related molecule that plays a role in gamma-radiation-induced cell cycle arrest. *Journal of Biological Chemistry* 277 (16): 13873–13882.
10. Bloem, L. J., T. R. Pickard, S. Acton, et al. 2001. Tissue distribution and functional expression of a cDNA encoding a novel mixed lineage kinase. *Journal of Molecular and Cellular Cardiology* 33 (9): 1739–1750.
11. Vind, A. C., A. V. Genzor, and S. Bekker-Jensen. 2020. Ribosomal stress-surveillance: Three pathways is a magic number. *Nucleic Acids Research* 48 (19): 10648–10661.
12. Wang, X., M. M. Mader, J. E. Toth, et al. 2005. Complete inhibition of anisomycin and UV radiation but not cytokine induced JNK and p38 activation by an aryl-substituted dihydropyrrolopyrazole quinoline and mixed lineage kinase 7 small interfering RNA. *Journal of Biological Chemistry* 280 (19): 19298–19305.
13. Jandhyala, D. M., A. Ahluwalia, T. Obrig, et al. 2008. ZAK: A MAP3Kinase that transduces Shiga toxin- and ricin-induced proinflammatory cytokine expression. *Cellular Microbiology* 10 (7): 1468–1477.
14 Vind, A. C., G. Snieckute, M. Blasius, et al. 2020. ZAKalpha Recognizes Stalled Ribosomes through Partially Redundant Sensor Domains. *Molecular cell* 78 (4): 700–13 e7.
15. Vind, A. C., G. Snieckute, S. Bekker-Jensen, et al. Run, Ribosome, Run: From compromised translation to human health . Antioxid Redox Signal, 2023.
16 Wu, C. C., A. Peterson, B. Zinshteyn, et al. 2020. Ribosome Collisions Trigger General Stress Responses to Regulate Cell Fate. *Cell* 182 (2): 404–16 e14.
17. Stoneley, M., R. F. Harvey, T. E. Mulroney, et al. 2022. Unresolved stalled ribosome complexes restrict cell-cycle progression after genotoxic stress. *Molecular Cell* 82 (8): 1557–72 e7.
18. Snieckute, G., L. Ryder, A. C. Vind, et al. 2023. ROS-induced ribosome impairment underlies ZAKalpha-mediated metabolic decline in obesity and aging. *Science* 382 (6675): eadf3208.
19. Snieckute, G., A. V. Genzor, A. C. Vind, et al. 2022. Ribosome stalling is a signal for metabolic regulation by the ribotoxic stress response. *Cell Metabolism* 34 (12): 2036–2046.
20. Sauter, K. A., E. A. Magun, M. S. Iordanov, et al. 2010. ZAK is required for doxorubicin, a novel ribotoxic stressor, to induce SAPK activation and apoptosis in HaCaT cells. *Cancer Biology & Therapy* 10 (3): 258–266.
21. Robinson, K. S., G. A. Toh, P. Rozario, et al. 2022. ZAKalpha-driven ribotoxic stress response activates the human NLRP1 inflammasome. *Science* 377 (6603): 328–335.
22. Robinson, K. S., G. A. Toh, M. J. Firdaus, et al. 2023. Diphtheria toxin activates ribotoxic stress and NLRP1 inflammasome-driven pyroptosis. *Journal of Experimental Medicine* 220 (10): e20230105.
23. Rozario, P., M. Pinilla, L. Gorse, et al. 2024. Mechanistic basis for potassium efflux-driven activation of the human NLRP1 inflammasome. *Proceedings of the National Academy of Sciences USA* 121 (2): e2309579121.
24. Song, H., B. Liu, W. Huai, et al. 2016. The E3 ubiquitin ligase TRIM31 attenuates NLRP3 inflammasome activation by promoting proteasomal degradation of NLRP3. *Nature Communications* 7: 13727.
25. Sann, H., J. Erichsen, M. Hessmann, et al. 2013. Efficacy of drugs used in the treatment of IBD and combinations thereof in acute DSS-induced colitis in mice. *Life Sciences* 92 (12): 708–718.
26. Hu, X., J. Deng, T. Yu, et al. 2019. ATF4 Deficiency Promotes Intestinal Inflammation in Mice by Reducing Uptake of Glutamine and Expression of Antimicrobial Peptides. *Gastroenterology* 156 (4): 1098–1111.
27. He, C., T. Yu, Y. Shi, et al. 2017. MicroRNA 301A Promotes Intestinal Inflammation and Colitis-Associated Cancer

Development by Inhibiting BTG1. *Gastroenterology* 152 (6): 1434–48 e15.
28. Mathea, S., K. R. Abdul Azeez, E. Salah, et al. 2016. Structure of the Human Protein Kinase ZAK in Complex with Vemurafenib. *ACS Chemical Biology* 11 (6): 1595–1602.
29. Park, S. H., J. Kim, and Y. Moon. 2020. Caveolar communication with xenobiotic-stalled ribosomes compromises gut barrier integrity. *Communications Biology* 3 (1): 270.
30. Jenster, L. M., K. E. Lange, S. Normann, et al. 2023. P38 kinases mediate NLRP1 inflammasome activation after ribotoxic stress response and virus infection. *Journal of Experimental Medicine* 220 (1): e20220837.
31. Wei, X., F. Xie, X. Zhou, et al. 2022. Role of pyroptosis in inflammation and cancer. *Cellular & Molecular Immunology* 19 (9): 971–992.
32. Yu, P., X. Zhang, N. Liu, et al. 2021. Pyroptosis: Mechanisms and diseases. *Signal Transduction and Targeted Therapy* 6 (1): 128.
33. Liu, Y. Q., Z. L. Hong, L. B. Zhan, et al. 2016. Wedelolactone enhances osteoblastogenesis by regulating Wnt/beta-catenin signaling pathway but suppresses osteoclastogenesis by NF-kappaB/c-fos/NFATc1 pathway. *Science and Reports* 6: 32260.
34. Shoemaker, C. J., and R. Green. 2012. Translation drives mRNA quality control. *Nature Structural & Molecular Biology* 19 (6): 594–601.
35. Bengtson, M. H., and C. A. Joazeiro. 2010. Role of a ribosome-associated E3 ubiquitin ligase in protein quality control. *Nature* 467 (7314): 470–473.
36. Zhao, M., Y. Wang, L. Li, et al. 2021. Mitochondrial ROS promote mitochondrial dysfunction and inflammation in ischemic acute kidney injury by disrupting TFAM-mediated mtDNA maintenance. *Theranostics* 11 (4): 1845–63.
37. Zhao, J., W. Gao, X. Cai, et al. 2019. Nanozyme-mediated catalytic nanotherapy for inflammatory bowel disease. *Theranostics* 9 (10): 2843–2855.
38 Maik-Rachline, G., E. Zehorai, T. Hanoch, et al. 2018. The nuclear translocation of the kinases p38 and JNK promotes inflammation-induced cancer. *Science Signaling* 11 (525): eaao3428.
39. Miranda, P. M., G. De Palma, V. Serkis, et al. 2018. High salt diet exacerbates colitis in mice by decreasing Lactobacillus levels and butyrate production. *Microbiome* 6 (1): 57.
40. Zhu, L., Z. Xie, G. Yang, et al. 2024. Stanniocalcin-1 Promotes PARP1-Dependent Cell Death via JNK Activation in Colitis. *Advanced Science (Weinh)* 11 (5): e2304123.
41. Zhang, Q., X. Su, C. Zhang, et al. 2023. Klebsiella pneumoniae Induces Inflammatory Bowel Disease Through Caspase-11-Mediated IL18 in the Gut Epithelial Cells. *Cellular and Molecular Gastroenterology and Hepatology* 15 (3): 613–632.
42. Xu, Y., X. Tang, A. Fang, et al. 2022. HucMSC-Ex carrying miR-203a-3p.2 ameliorates colitis through the suppression of caspase11/4-induced macrophage pyroptosis. *International Immunopharmacology* 110: 108925.
43. Oficjalska, K., M. Raverdeau, G. Aviello, et al. 2015. Protective role for caspase-11 during acute experimental murine colitis. *The Journal of Immunology* 194 (3): 1252–1260.
44. Williams, T. M., R. A. Leeth, D. E. Rothschild, et al. 2015. Caspase-11 attenuates gastrointestinal inflammation and experimental colitis pathogenesis. *American Journal of Physiology. Gastrointestinal and Liver Physiology* 308 (2): G139–G150.
45. Blazejewski, A. J., S. Thiemann, A. Schenk, et al. 2017. Microbiota Normalization Reveals that Canonical Caspase-1 Activation Exacerbates Chemically Induced Intestinal Inflammation. *Cell Reports* 19 (11): 2319–2330.
46. Demon, D., A. Kuchmiy, A. Fossoul, et al. 2014. Caspase-11 is expressed in the colonic mucosa and protects against dextran sodium sulfate-induced colitis. *Mucosal Immunology* 7 (6): 1480–1491.
47. Fan, T. J., S. Y. Tchaptchet, D. Arsene, et al. 2018. Environmental Factors Modify the Severity of Acute DSS Colitis in Caspase-11-Deficient Mice. *Inflammatory Bowel Diseases* 24 (11): 2394–2403.
48. Stone, S. M., C. M. Thorpe, A. Ahluwalia, et al. 2012. Shiga toxin 2-induced intestinal pathology in infant rabbits is A-subunit dependent and responsive to the tyrosine kinase and potential ZAK inhibitor imatinib. *Frontiers in Cellular and Infection Microbiology* 2: 135.
49. Wang, Y., Z. Fu, X. Li, et al. 2021. Cytoplasmic DNA sensing by KU complex in aged CD4(+) T cell potentiates T cell activation and aging-related autoimmune inflammation. *Immunity* 54 (4): 632–47 e9.